Draft version April 3, 2008
Preprint typeset using LaTeX style emulateapj v. 10/09/06

COSMIC EVOLUTION OF BLACK HOLES AND SPHEROIDS. III. THE M_{BH}-σ_* RELATION IN THE LAST SIX BILLION YEARS

Jong-Hak Woo[1], Tommaso Treu[1,2], Matthew A. Malkan[3], Roger D. Blandford[4]

Draft version April 3, 2008

ABSTRACT

We measure the evolution of the correlation between black hole mass and host spheroid velocity dispersion (M_{BH}-σ_*) over the last 6 billion years, by studying three carefully selected samples of active galaxies at $z = 0.57$, $z = 0.36$ and $z < 0.1$. For all three samples, virial black hole masses are consistently estimated using the line dispersion of Hβ and the continuum luminosity at 5100Å or Hα line luminosity, based on our cross calibration of the broad line region size-luminosity relation. For the $z = 0.57$ sample, new stellar velocity dispersions are measured from high signal-to-noise ratio spectra obtained at the Keck Telescope, while for the two lower redshift samples they are compiled from previous works. Extending our previous result at $z = 0.36$, we find an offset from the local relation, suggesting that for fixed M_{BH}, distant spheroids have on average smaller velocity dispersions than local ones. The measured offset at $z = 0.57$ is $\Delta \log \sigma_* = 0.12 \pm 0.05 \pm 0.06$ (or $\Delta \log M_{BH} = 0.50 \pm 0.22 \pm 0.25$), i.e. $\Delta \log M_{BH} = (3.1 \pm 1.5) \log(1 + z) + 0.05 \pm 0.21$. This is inconsistent with a tight and non-evolving universal M_{BH}-σ_* relation at the 95%CL.

Subject headings: accretion, accretion disks — black hole physics — galaxies: active — galaxies: evolution — quasars: general

1. INTRODUCTION

Understanding the origin of the black hole mass - spheroid velocity dispersion (M_{BH}-σ_*) relation (Ferrarese & Merritt 2000; Gebhardt et al. 2000) is a key goal of unified models of black hole – galaxy coevolution (e.g. Kauffmann & Haenhelt 2000; di Matteo et al. 2005; Ciotti & Ostriker 2007). One of the most powerful observational tests of the proposed explanations is to measure the time evolution of the M_{BH}-σ_* relation since various scenarios predict different cosmic evolution. For example, – for a fixed M_{BH} – Robertson et al. (2006) predict an increase of σ_* with redshift, Croton (2006) and Bower et al. (2006) predict a decrease, while Granato et al. (2004) expect no evolution.

In recent years, a number of groups have investigated the evolution of the M_{BH}-σ_* relation, using various techniques to estimate σ_* of AGN host galaxies (e.g. Shields et al. 2003; Walter et al. 2004; Salviander et al. 2007). Starting with our pilot study (Treu et al. 2004), we reported the first direct measurement of the M_{BH}-σ_* relation beyond the local Universe (Woo et al. 2006, hereafter paper I), and updated it with corrected AGN continuum luminosities using Hubble Space Telescope (HST) images in paper II (Treu et al. 2007).

By observing 14 Seyfert 1 galaxies, we determined stellar velocity dispersions in the integrated spectra, and M_{BH} from AGN broad emission line widths, which are thought to measure the gravity of the central mass on sub-parsec scales. We found that the measured M_{BH}-σ_* relation at $z = 0.36$ is offset with respect to the local relationship ($\Delta \log M_{BH} = 0.54 \pm 0.12 \pm 0.21$ at fixed σ_*). In other words black holes of a fixed mass appeared to live in bulges with smaller velocity dispersion 4 Gyrs ago (at 95% CL), consistent with recent growth and evolution of intermediate mass spheroids. Using HST images, we obtained a consistent result, $\Delta \log M_{BH} > 0.51 \pm 0.14 \pm 0.17$, by measuring the M_{BH}- spheroid luminosity relation of the same sample (paper II). This result may be consistent with a scenario where intermediate-mass blue galaxies undergo merging at relatively recent times and arrive on the local black hole-galaxy relations by becoming more massive red galaxies. However, much work remains to be done due to the small sample size and large uncertainties, before this initial result can become a high precision measurement.

We report here our first measurement at the next redshift window ($z = 0.57$, adding ∼50% to the look-back time), so that evolutionary trends can be measured over a longer range in cosmic time. We also improve the local baseline by consistently estimating M_{BH} for a sample of 48 nearby Seyfert 1 galaxies with published stellar velocity dispersion (Greene & Ho 2006). To minimize repetition, readers are referred to our previous works (papers I, II; McGill et al. 2008; hereafter M08) for detailed discussions of the systematics inherent to the measurement. The paper is organized as follows. Section 2 describes sample selection and observations. Section 3 presents our measurements. Section 4 presents the M_{BH}-σ_* relation. Discussion and conclusions are presented in § 5. We adopt $\Omega_m = 0.3$, $\Omega_\Lambda = 0.7$, and $H_0 = 70$ km sec^{-1} Mpc^{-1}.

2. DATA

A sample of broad-line AGNs was selected from the Sloan Digital Sky Survey Data Release 4 (SDSS DR4). Following our strategy at $z = 0.36 \pm 0.01$ (paper I), we chose the next redshift window, $z = 0.57 \pm 0.01$, to avoid strong sky features on the redshifted stellar lines around the Mg-Fe line region, minimizing the uncertainties re-

[1] Department of Physics, University of California, Santa Barbara, CA 93106-9530; woo@physics.ucsb.edu, tt@physics.ucsb.edu
[2] Sloan Fellow, Packard Fellow
[3] Department of Physics and Astronomy, University of California at Los Angeles, CA 90095-1547, malkan@astro.ucla.edu
[4] Kavli Institute for Particle Astrophysics and Cosmology, Stanford, CA, rdb@slac.stanford.edu

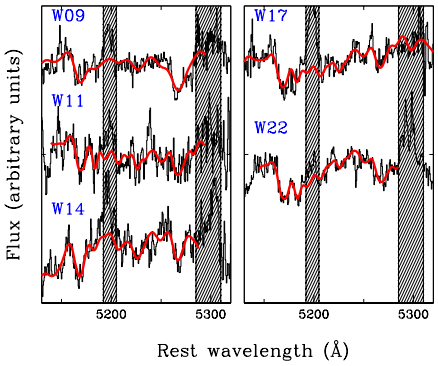

FIG. 1.— Velocity dispersion measurements. The region including the main stellar features is shown together with the best fit template (red thick line). The regions around narrow AGN emission lines – identified by vertical lines – are masked out before fitting.

lated to sky subtraction and atmospheric absorption corrections.

Our selection procedure was slightly modified with respect to that of the lower redshift sample. Initially, 365 broad-line AGNs at z=0.57±0.01 were collected from SDSS DR4, based on the presence of the broad Hβ line. Out of 365 AGNs, we selected 20 objects with g'-r'>0.1 and r'-i'>0.3 (AB), expecting non-negligible stellar light in the observed spectra, based on stellar and AGN spectral models. The effects of this color cut will be modeled in detail in future papers, when Keck and possibly HST data for a larger sample at $z = 0.57$ will be available. However, since the colors of the new sample are similar to those of the $z = 0.36$ sample, we do not expect the color cut to introduce a significant bias. In any case, the color cut will tend to select more massive host galaxies for a given nuclear luminosity. Hence, if any biased is introduced, it should bias against the offset seen in papers I and II.

High signal-to-noise (S/N) ratio spectra for 5 objects were obtained with the LRIS spectrograph (Oke et al. 1995) at the Keck-I telescope during two runs in January 2007 and April 2007. The 831 lines mm^{-1} grating centered at 7600Å was used with a 1" wide slit, yielding a pixel scale of 0.92Å×0.″215 and a Gaussian resolution (σ) ∼58 km s^{-1}. Observing conditions were generally favorable with 0.7-1.2" seeing. Total exposure times for each object ranges between 2.5 and 3.5 hours. The observing strategy, data reduction, calibration, and one-dimensional spectra extraction processes were very similar to those described in paper I.

3. MEASUREMENTS

This section describes our measurement of σ_* and M_{BH} for the 5 Seyferts at $z = 0.57$ (§ 3.1 and § 3.2), and M_{BH} estimates for the 48 local Seyferts (§ 3.3). The relevant properties of the $z = 0.57$ sample are listed in Table 1.

3.1. *Stellar Velocity Dispersion*

We used the Mg-Fe region (rest-frame ∼ 5050-5300Å) to measure velocity dispersion as described in detail in paper I. Here, we briefly summarize the procedure and systematic uncertainties. First, we subtracted broad AGN Fe emission, using a set of I Zw 1 templates. Then, we compared in pixel space the observed spectra with 5 stellar templates (G8, G9, K0, K2, and K5 giant) broadened with a range of Gaussian velocity. AGN narrow emission lines (e.g. [N I] 5201Å and [Fe XIV] 5304Å) were masked out before fitting, as shown in Figure 1. Fits were performed for all templates to estimate the effect of template mismatch, yielding comparable measurements within the errors (10-20%). The best-fit template was used for the final dispersion measurements.

The Mg-Fe region typically used for dynamical studies is a natural choice for our sample since other strong stellar features such as the CaII triplet are out of the optical spectral range. Feature mismatch due to α-enhancement in massive early-type galaxies is a well-known problem in kinematics studies (e.g. Barth et al. 2003; Woo et al. 2004) and can potentially increase systematic uncertainties. However, in paper I we found that only one out of 14 Seyfert galaxies at $z = 0.36$ shows signs of Mg mismatch, as expected because the inferred stellar velocity dispersions are more typical of a Milky Way type galaxy than of a massive early-type galaxy. As for the lower redshift sample, we do not find significant mismatch in our $z = 0.57$ sample, as shown in Figure 1.

Following the procedure described in paper I, we estimate a total systematic uncertainty of 0.05 dex on σ, combining the effects of template mismatch, potential errors due to the large spectroscopic aperture, and host galaxy morphology and inclination. This translates into 0.20 dex uncertainty of the offset in log M_{BH} from the M_{BH}-σ_* relation.

3.2. *Black Hole Mass*

Black hole mass can be estimated using the 'virial' method based on the empirical relation between the size of the broad line region and continuum luminosity of the reverberation sample (Kaspi et al. 2005), and the velocity scale given by the width of the broad emission lines. In practice, we measured the line dispersion of broad Hβ by fitting the observed line profile with Gauss-Hermite polynomials as described in paper I and in M08. The continuum luminosity around 5100Å (L_{5100}) was measured by averaging flux in the 5070-5130Å region. Considering the difficulty of achieving absolute flux calibration for the Keck spectra – due to slit losses, variable seeing and sky transparency– we re-calibrated our spectrophotometry with the extinction corrected i' band magnitude taken from the SDSS-DR6 archive, by calculating and correcting for the offset between Sloan and our synthetic i' band magnitude measured from the observed spectra.

For low luminosity AGNs ($L_{5100} < 10^{44}$ erg s^{-1}) continuum luminosity can be overestimated due to the significant contribution from host galaxies. Thus, correcting for the host galaxy contamination is crucial to avoid overestimation of M_{BH}. The size-luminosity relation was in fact revised with a lower slope (∼0.5 as expected in photoionization scenarios) and a higher normalization, after correcting for the galaxy contamination in low luminosity AGNs in the reverberation sample (Bentz et al. 2006a).

It requires high resolution HST imaging to correct for the host galaxy contamination for distant AGNs. Since this is not available for our sample at the moment, we cannot but adopt the size-luminosity relation based on the total (observed) luminosity. However, based on our

TABLE 1
Targets and Measured Properties

Name	z	RA (J2000)	DEC (J2000)	i' mag	Exp. hr	S/N Å^{-1}	$\sigma_{H\beta}$ km s^{-1}	λL_{5100} 10^{44} erg s^{-1}	log $M_{BH}/M_\odot$	σ_* km s^{-1}
(1)	(2)	(3)	(4)	(5)	(6)	(7)	(8)	(9)	(10)	(11)
W9	0.5651	15 52 27.82	+56 22 36.47	19.00	2.5	79	2598	4.31	8.64	289± 19
W11	0.5649	1 55 16.18	-9 45 55.99	20.03	3	32	2103	1.53	8.15	126± 21
W14	0.5616	12 56 31.90	-2 31 30.62	18.71	2.5	94	2192	4.94	8.54	228± 20
W17	0.5611	10 07 28.38	+39 26 51.83	19.71	2.5	32	2320	2.00	8.31	165± 14
W22	0.5649	3 42 29.70	-5 23 19.49	18.60	3.5	101	2442	5.77	8.68	144± 21

Note. — Col. (1): Target ID. Col. (2): Redshift from SDSS-DR6. Col. (3): Right Ascension. Col. (4): Declination. Col. (5): Extinction corrected i' AB magnitude from SDSS photometry. Col. (6): Total exposure time. Col. (7): Signal-to-noise ratio of the combined spectrum (average in the 8000-8300Åspectral region). Col. (8): Second moment of Hβ in km s^{-1}. Typical error is ∼10%. Col. (9): Rest frame luminosity at 5100Å. Typical error is a few %. Col. (10): Logarithm of M_{BH} in solar units. Estimated uncertainty is 0.4 dex. Col. (11): Stellar velocity dispersion.

experience at $z = 0.36$, host galaxy contamination is not expected to be a major effect. In paper II, for Seyfert galaxies with similar luminosity, we compared M_{BH} estimates based on the size-luminosity relation of Kaspi et al. (2005) with new estimates based on the revised size-luminosity relations of Bentz et al. (2006a), after correcting for host galaxy contamination using HST images. We found that new M_{BH} estimates are on average 0.09 dex smaller, due to the combined effects of removing host galaxy light while using the new size-luminosity relation with a higher normalization.

Therefore, we will adopt as our best estimate of M_{BH}, the following equation from Paper I based on Kaspi et al. (2005) and Onken et al. (2004), equivalent to the most recent calibration of empirical M_{BH} estimators from M08:

$$M_{\rm BH} = 10^{8.33}{\rm M}_\odot \times \left(\frac{\sigma_{H\beta}}{3000{\rm kms}^{-1}}\right)^2 \left(\frac{\lambda L_{5100}}{10^{44}{\rm ergs}^{-1}}\right)^{0.69}, \quad (1)$$

where $\sigma_{H\beta}$ is the line dispersion (second moment) of Hβ. We assume 0.4 dex uncertainty on the estimated M_{BH}, based on comparisons of reverberation data and single-epoch data (Vestergaard & Peterson 2006; M08), which dominates the errors on $\sigma_{H\beta}$ and L_{5100}.

As a sanity check, we compared M_{BH} estimates based on Equation 1 with those based on the new size-luminosity relation (Bentz et al. 2006a) along with the same virial coefficient of Onken et al. (2004):

$$M_{\rm BH} = 10^{8.58}{\rm M}_\odot \times \left(\frac{\sigma_{H\beta}}{3000{\rm kms}^{-1}}\right)^2 \left(\frac{\lambda L_{5100,n}}{10^{44}{\rm ergs}^{-1}}\right)^{0.518}, \quad (2)$$

where $L_{5100,n}$ is the *nuclear* luminosity at 5100Å after correcting for host galaxy contamination. Since high resolution images needed for an accurate measurement of the nuclear luminosity are not available for our sample, we assume an average AGN fraction in the observed light at 5100Å. If the host galaxy contamination is negligible ($L_{5100,n}$= L_{5100}), Equation 2 gives 0.16 dex higher M_{BH} compared to Equation 1, while if the AGN fraction is assumed to be 50%, M_{BH} is 0.006 dex higher. Thus, using Equation 1 without correcting for the host galaxy contamination – which we cannot do at the moment – does not significantly affect our M_{BH}estimates. As in paper I, we adopt a systematic error of 0.11 dex in M_{BH} estimates, which is dominated by AGN continuum luminosity uncertainty due to host galaxy contamination.

3.3. *Local Seyferts*

To measure the evolution of the M_{BH}-σ_* relation, it is important to have a well defined local sample. The sample of 14 Seyfert galaxies with reverberation M_{BH}, and measured stellar velocity dispersion (Onken et al. 2004) is a good local benchmark. However, it is desirable to have a complementary sample for two reasons. First, the reverberation sample is small in size and shows a flattened distribution on the M_{BH}-σ_* plane, especially with a new reverberation black hole mass of NGC 4151 (Bentz et al. 2006b; see magenta points in Figure 2). Second, there could be an unknown systematic offset between the reverberation mass and our single-epoch mass due to the uncertainties in measuring velocity and luminosity from single-epoch spectra, potentially caused by, e.g., flux variability, velocity variability, the narrow line subtraction (e.g. Collin et al. 2006; Woo 2008).

For these reasons, we estimated M_{BH} for a sample of local Seyferts, using the line dispersion of Hβ and Hα line luminosity ($L_{H\alpha}$), and a formula consistently calibrated with that used for M_{BH} estimates at $z = 0.36$ and $z = 0.57$ (M08). We selected 55 Seyfert 1 galaxies at $z < 0.1$ from SDSS-DR6, with published stellar velocity dispersion (Greene & Ho 2006). Seven objects were excluded due to the very faint broad component of Hβ that prevented us from measuring reliable line widths. For local low luminosity Seyferts, host galaxy light is a significant fraction of the light observed within the Sloan fiber (3" diameter), superimposing strong stellar absorption on the broad Hβ line profile. Thus, we subtracted the stellar features, using eigenspectra templates based on a principal component analysis of several hundred galaxy spectra (Hao et al. 2005). Since the L_{5100} measured from SDSS spectra could be also significantly contaminated by stellar light, we used $L_{H\alpha}$ from Greene & Ho (2006) instead, together with the M_{BH} recipe calibrated by M08 and Green & Ho (2005).

4. THE M_{BH}-σ_* RELATION

In Figure 2, the M_{BH}-σ_* relation for local active galaxies (left panel) and our samples at $z = 0.36$ and $z = 0.57$ (right panel) are presented along with local quiescent galaxies. Two local AGN samples (SDSS sample from § 3.3 and the reverberation sample from Onken et al. 2004) are consistent with the M_{BH}-σ_* relation of quiescent galaxies, although the scatter is somewhat larger (r.m.s. 0.45 and 0.43 dex, respectively for the SDSS

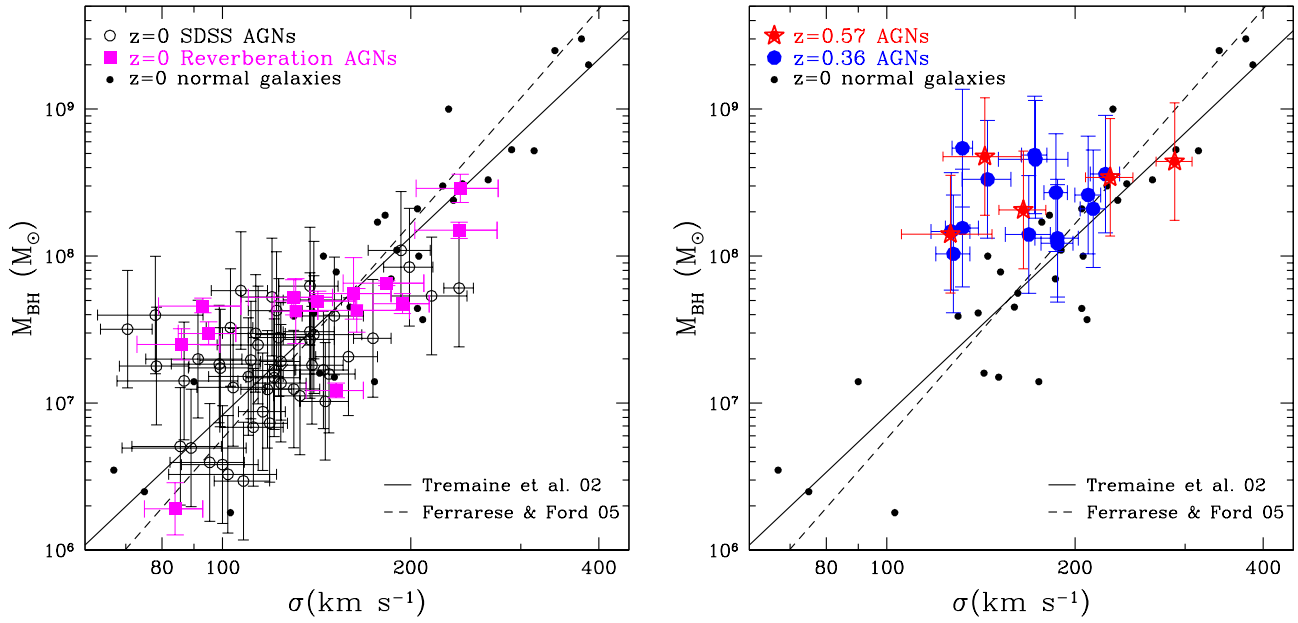

FIG. 2.— The M_{BH}-σ_* relation of active galaxies. Left panel: local Seyferts with σ_* from Greene & Ho (2006) and our own M_{BH} estimates, consistently calibrated with our estimates for distant samples (black circles); local Seyferts with M_{BH}, measured via reverberation mapping (Onken et al. 2004; magenta squares). Right panel: new measurements at $z = 0.57$ (red stars); Seyfert galaxies at $z = 0.36$ from our earlier work (paper I, II; blue circles). The local relationships of quiescent galaxies (Tremaine et al. 2002; black points) are shown for comparison as a solid (Tremaine et al. 2002) and dashed (Ferrarese & Ford 2005) line.

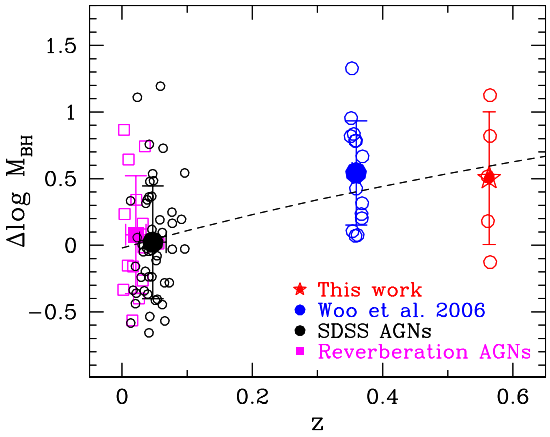

FIG. 3.— Offset in M_{BH} with respect to the local quiescent sample (Tremaine et al. 2002) as a function of redshift. Large solid points with error bars represent the average and rms scatter for the four samples of active galaxies. The rms scatter of the $z = 0.57$ sample is 0.5 dex, similar to that of local active galaxies. Note that all 'virial' M_{BH} are based on the second moment of Hβ and the same calibration of the virial coefficient. The dashed line represent the best fit relation $\Delta \log M_{BH} = (3.1 \pm 1.5) \log(1+z) + 0.05 \pm 0.21$.

sample and the reverberation sample) compared to that of quiescent galaxies (∼0.3 dex). The scatter increases as galaxy mass decreases, perhaps consistent with mass-dependent evolution in the sense that less massive galaxies are still evolving to the M_{BH}-σ_* relation. This may indicate that the M_{BH}-σ_* relation is not as tight for late-type galaxies even at $z \sim 0$. Splitting evenly the local sample into two groups below and above $\sigma_* = 120$km s^{-1}, and taking into account the measurement errors on σ_*, we find that the intrinsic scatter is a factor of 2 larger for the low σ_* sample (0.43 vs 0.22).

The distant samples are offset from the local M_{BH}-σ_* relation. The average offset of the $z = 0.57$ sample is $0.50 \pm 0.22 \pm 0.25$ dex in M_{BH}, corresponding to $0.12 \pm 0.05 \pm 0.06$ in $\log \sigma_*$ – in the sense that velocity dispersions were on average smaller for given M_{BH} six Gyrs ago (Figure 3). Using the new size-luminosity relation of Bentz et al. 2006a (Equation 2) and assuming an average AGN fraction ∼50%, we find an equivalent offset, ΔlogM_{BH}= 0.51. If the AGN fraction is higher, then the offset increases (see Section 3.2), indicating that M_{BH} estimates based on Equation 1 is not significantly overestimated. The result is similar to the average offset of the $z = 0.36$ sample (papers I and II), although the error bars on the measurement are large enough to allow for a variety of redshift trends. We include in our error analysis, in addition to the random errors, a potential systematic error of 0.25 dex, estimated by combining systematic uncertainties in M_{BH} and σ_*.

To quantify the significance of evolution, we consider the three active samples. We emphasize that M_{BH} was consistently estimated based on the line dispersion of Hβ and the same virial coefficient (shape factor). Thus, a change in the virial coefficient will move all samples vertically by the same amount, keeping the offset unchanged, unless the kinematics of the broad line region (hence, the virial coefficient) varies as a function of M_{BH} or redshift. Therefore, we consider the systematic error on the relative calibration of M_{BH} to be negligible, leaving systematic errors in the measurement of σ_* as the main source of systematic uncertainty in the evolution. Including random and systematic errors in the analysis, we find that the best fit relation is $\Delta \log M_{BH} = (3.1 \pm 1.5) log(1 + z) + (0.05 \pm 0.21)$, i.e. the slope is non zero at the two sigma level. However, as discussed in paper I and II, it is important to keep in

mind that the observed offset may not represent evolution, if the higher z samples are not direct progenitors of the lower z samples due to, e.g., the somewhat different scales in galaxy mass and M_{BH}.

5. DISCUSSION AND CONCLUSIONS

We investigated the evolution of the M_{BH}-σ_* relation using three samples of Seyfert galaxies at $z < 0.1$, $z = 0.36$, and $z = 0.57$, finding evolution in the last 6 Gyr at the 95%CL. This result is consistent with a scenario where black hole growth predates bulge assembly and that bulges grow substantially in the last 6 Gyr – at least at this mass scale – if the local M_{BH}-σ_* relation is the universal end-point of black hole-galaxy coevolution.

As discussed in paper I, collisional merging of late-type galaxies can drive the evolution of the M_{BH}-σ_* relation. The mass and stellar velocity dispersion of the final spheroid will increase, not only by forming new stars but also transforming rotation-supported disk stars into pressure-supported spheroid components. This can potentially overcome the growth in M_{BH} due to merging with the supermassive black hole of the companion, especially if the companion galaxy is not spheroid dominated.

In a galaxy merging scenario, the evolution of the M_{BH}-σ_* relation could be mass-dependent, similarly to the downsizing trends in galaxy evolution (Cowie et al. 1996) and AGN evolution (Barger et al. 2005). As seen for example in fundamental plane studies (e.g. Treu et al. 2005, Woo et al. 2004, 2005), active and quiescent massive early-type galaxies have relatively old stellar populations in the redshift range considered here ($z \sim 0.4-0.6$). Together with the results on the evolution of the mass function (e.g. Bundy et al. 2007), this is consistent with an early epoch of assembly for the most massive spheroids. Thus, the evolution of the M_{BH}-σ_* relation could be mass dependent, slower at this redshift for the more massive galaxies (see Peng et al. 2006 for the M_{BH}–spheroid luminosity relation of massive high redshift galaxies, which show evolution in the same sense as our sample since z∼2). Recently, Shen et al. (2008) present the M_{BH}-σ_*relation out to $z \sim 0.4$ based on SDSS spectra, concluding that the offset (in the same direction as the one reported here) with redshift is not significant for their sample. However, since their 28 galaxies with measured σ_* at z>0.3 have an average S/N=18.7 per pixel (and hence the S/N of the stellar spectrum is less than ∼10 per pixel if the nuclear light fraction is ∼50%) and M_{BH} was based on the FWHM of Hβ line, direct comparison with our result is not straightforward. As discussed in paper II, the broad observational picture is far from conclusive at the moment, requiring larger samples over a wider mass range than the present sample to test this hypothesis.

It is important to consider selection effects. First, since our samples were selected based on the flux and width of the broad lines, they could be biased towards high M_{BH} objects (paper II; see also Lauer et al. 2007b). However, as we showed in paper II with Monte Carlo simulations, this bias is too small to account for the observed offset[5], unless the intrinsic scatter of the M_{BH}-σ_* relation at $z = 0.57$ – which is unknown – is of order 1 dex. Second, although active galaxies are the only target for M_{BH} estimation in the distant universe, they may not represent the general galaxy population, as they are rare objects with a highly accreting and radiatively efficient black hole. However, two pieces of evidence argue against the explanation of the observed evolution purely in terms of systematic differences between active and quiescent galaxies: i) a consistent M_{BH}-σ_* relation is found locally for the two active galaxy samples; ii) the M_{BH}-σ_* of distant active galaxies is offset from that of the local active sample.

An alternative or complementary explanation of the observed offset is that the M_{BH}-σ_* relation is not tight for late-type galaxies, as perhaps suggested by the increasing scatter for local active samples, especially at the low mass end. This scenario is consistent with the idea of downsizing, with low mass blue late type-galaxies yet to join the more massive red early-type galaxies on the tight M_{BH}-σ_* relation. So far, only a few late-type galaxies are included in the local quiescent galaxy sample that defines the local M_{BH}-σ_* relation. A larger sample with more disk-dominant quiescent galaxies is needed to investigate any systematic difference in the local scaling relations.

This work is based on data collected at the Keck Observatory, operated by Caltech, UC, and NASA, and is made possible by the public archive of the Sloan Digital Sky Survey. T.T. acknowledges support from the NSF through CAREER award NSF-0642621, from the Sloan Foundation, and from the Packard Foundation. We acknowledge financial support from NASA through HST grant AR-10986. We thank C. Peng and M. Favata for useful discussions, L. Hao for providing the PCA algorithm, and the referee for useful suggestions.

[5] The M_{BH} range and measured offset are similar to those of the sample studied in paper II, resulting in the same negligible bias < 0.1 dex.

REFERENCES

Barger, A. J., Cowie, L. L., Mushotzky, R. F., Yang, Y., Wang, W.-H., Steffen, A. T., & Capak, P. 2005, AJ, 129, 578
Bentz, M. C., Peterson, B. M., Pogge, R. W., Vestergaard, M., & Onken, C. A. 2006a, ApJ, 644, 133
Bentz, M. C., et al. 2006b, ApJ, 651, 775
Bower, R. G., et al. 2006, MNRAS, 370, 645
Bundy, K., Treu, T., & Ellis, R. S. 2007, ApJ, 665, L5
Ciotti, L., & Ostriker, J. P. 2007, ApJ, 665, 1038
Collin, S., Kawaguchi, T., Peterson, B. M., & Vestergaard, M. 2006, A&A, 456, 75
Cowie, L. L., Songaila, A., Hu, E. M., & Cohen J. G. 1996, AJ, 112, 839
Croton, D. J. 2006, MNRAS, 369, 1808
Di Matteo, T., Springel, V., & Hernquist, L. 2005, Nature, 433, 604
Ferrarese, L., & Merritt, D. 2000, ApJ, 539, L9
Ferrarese, L. & Ford, H. 2005, Space Science Reviews, 116, 523
Gebhardt, K., et al. 2000, ApJ, 539, L13
Granato, G. L., De Zotti, G., Silva, L., Bressan, A., & Danese, L. 2004, ApJ, 600, 580
Greene, J. E., & Ho, L. C. 2005, ApJ, 630, 122
Greene, J. E., & Ho, L. C. 2006, ApJ, 641, L21
Hao, L., et al. 2005, AJ, 129, 1795

Hopkins, P. F., Somerville, R. S., Hernquist, L., Cox, T. J., Robertson, B., & Li, Y. 2006, ApJ, 652, 864
Kaspi, S., Maoz, D., Netzer, H., Peterson, B. M., Vestergaard, M., & Jannuzi, B. T. 2005, ApJ, 629, 61
Kauffmann, G., & Haehnelt, M. 2000, MNRAS, 311, 576
Lauer, T. R., et al. 2007a, ApJ, 662, 808
Lauer, T. R., Tremaine, S., Richstone, D., & Faber, S. M. 2007b, ApJ, 670, 249
McGill, K. L., Woo, J.-H., Treu, T., & Malkan, M. A. 2008, ApJ, 673, 703 (M08)
Onken, C. A., et al. 2004, ApJ, 615, 645
Peng, C. Y., Impey, C. D., Rix, H.-W., Kochanek, C. S., Keeton, C. R., Falco, E. E., Lehár, J., & McLeod, B. A. 2006, ApJ, 649, 616
Robertson, B., et al. 2006, ApJ, 641, 90
Salviander, S., Shields, G. A., Gebhardt, K., & Bonning, E. W. 2007, ApJ, 662, 131
Shen, J., Vanden Berk, D. E., Schneider, D. P., & Hall, P. B. 2008, AJ, 135, 928
Shields, G. A., et al. 2003, ApJ, 583, 124
Tremaine, S., et al. 2002, ApJ, 574, 740
Treu, T., Malkan, M., & Blandford, R. D. 2004, ApJ, 615, L97
Treu, T., Ellis, R. S., Liao, T. X., & van Dokkum, P. G. 2005, ApJ, 622, L5
Treu, T., Woo, J.-H., Malkan, M. A., & Blandford, R. D. 2007, ApJ, 667, 117 (paper II)
Vestergaard, M. & Peterson, B. M. 2006, ApJ, 641, 689
Walter, F., et al. 2004, ApJ, 615, L17
Woo, J.-H., Urry, C. M., Lira, P., van der Marel, R. P., & Maza, J. 2004, ApJ, 617, 903
Woo, J.-H., Urry, C. M., van der Marel, R. P., Lira, P., & Maza, J. 2005, ApJ, 631, 762
Woo, J.-H., Treu, T., Malkan, M. A., & Blandford, R. D. 2006, ApJ, 645, 900 (paper I)
Woo, J.-H. 2008, AJ, in press (astroph/0802.3705)